

New Organometallic Polymers by Polycondensation of Ferrocene and Siloxane Derivatives

Maria Cazacu,^{*,†} Angelica Vlad,[†] Mihai Marcu,[†] Carmen Racles,[†] Anton Airinei,[†] and Grigore Munteanu[‡]

“Petru Poni” Institute of Macromolecular Chemistry, Aleea Gr. Ghica Voda 41A, 700487, Iasi, Romania, and Chemistry Institute, Academy Street nr. 3, Moldavian Academy, Chishinew, Moldova MD-2028

Received September 19, 2005; Revised Manuscript Received March 24, 2006

ABSTRACT: A series of condensation polymers (polyesters and polyamides) of ferrocene and siloxane derivatives have been synthesized and characterized. Thus, 1,1'-di(chlorocarbonyl)ferrocene (CAFc) and four different siloxane derivatives—1,3-bis(aminopropyl)tetramethyldisiloxane (AP₀), α,ω -bis(3-aminopropyl)oligodimethylsiloxane (AP), 1,3-bis(hydroxypropyl)tetramethyldisiloxane (HP₀), and 1,3-bis(*p*-hydroxyphenyleneazomethine-3-propyl)tetramethyldisiloxane (HBS₀)—were used as monomers for this purpose. A model polyamide was prepared by polycondensation of oxalyl chloride with AP₀. This was analyzed as such or doped with ferrocene in order to appreciate the influence of the ferrocene units by comparison with the corresponding copolymer containing chemically linked ferrocene in the main chain. Thermal, mesomorphic, viscometric, and solubility behaviors of the obtained compounds were studied. Molecular masses were estimated by GPC. The polymers were investigated by cyclic voltammetry and UV–vis absorption spectroscopy in order to evaluate the redox properties and photochemical behavior.

Introduction

The incorporation of transition metals into a polymer chain offers potential for the preparation of processable materials with properties which significantly differ from those of conventional organic polymers. The diverse range of coordination numbers and geometries of the transition elements offers the possibility of accessing polymers with unusual conformational, mechanical, and morphological characteristics.^{1,2} Such polymers are of considerable interest in materials science because the presence of the metal atoms can also impart unique redox, electronic, optical, and magnetic properties.³

The widespread utility of organosiloxane polymers has led to an increasing interest in modification of their properties by incorporation of various moieties in the polymer chain. The chemical insertion of the metals in siloxane-based polymeric structures constitutes a challenge for obtaining materials with new properties, taking into account the polysiloxane's uniqueness. Thus, as is well-known, the polysiloxane is one of the most flexible polymers having low intermolecular forces, which are responsible for a low solubility parameter. They have very low surface energies, and therefore the materials on their basis are widely used as coatings, mold-release agents, surface modifiers, or separation membranes. The high free volume in the siloxanes, compared to hydrocarbons, confers a high gases diffusion coefficient. Another important property of polysiloxanes is their exceptional stability against heat, oxidation, and UV radiation.⁴ The high flexibility of the polymer backbone can cause changes in geometry of the polymer bound metal complex, which is an important parameter in the case of their use as catalyst.⁵ Their chemical and physiological inertness and high gas permeability makes them attractive in biomedicine.⁶

Iron, by far the cheapest and most abundant transition metal both in the crust of the earth and in the human and animal body, is remarkable by versatility of its oxidation state, reduction potential, coordination number, and spin state. The organometallic chemistry of iron is dominated by complexes that contain cyclopentadienyl and/or carbonyl ligands.⁷ Ferrocene is known as one of the most thermally stable organometallic compounds.⁸ The other properties that the ferrocenyl groups introduce into polymers have been investigated.⁹ It has been found that poly(ferrocenyl)-based macromolecules are of interest for their useful application in the chemical modification of electrodes, electrochemical sensors, and charge dissipation materials, which provide protection with respect to ionizing radiation such as electrons, materials for the construction of liquid crystals and nonlinear optical (NLO) systems, electronic devices, or chiral ligands for asymmetric catalysis. The magnetic properties of oxidized poly(ferrocenes) have attracted attention.^{1,10} Poly(ferrocene) block copolymers also allow access to nanostructured materials.¹

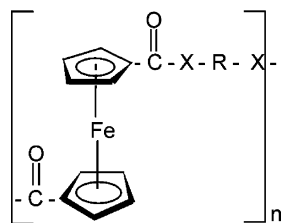
There are many reports on macromolecular systems containing the ferrocenyl moiety besides highly flexible dimethylsiloxane and more rigid organic¹¹ or silane sequences synthesized in general by transition-metal-catalyzed ring-opening polymerization of the ferrocenophane^{1,2,8,12,13} or by hydrosilylation of vinyl-functionalized ferrocene with methyl-H-siloxanes.^{10,14–16} The literature on the synthesis of siloxane–ferrocene macromolecular systems by the polycondensation procedure is very scarce.¹⁷ To our knowledge, only one report discussed the synthesis by polycondensation of siloxane-based polymeric structures in which the amide-linked ferrocenyl moieties are incorporated pendant or as a part of the polymer backbone.¹⁸ Like in the synthesis of ferrocene-containing polyamide and polyester derived from various organic diols and diamines,¹⁹ the difunctional ferrocene derivative, namely 1,1'-ferrocenedicarboxylic acid, was reacted with polysiloxanes end- or side-functionalized with aminopropyl groups.¹⁸ The same ferrocene

[†] “Petru Poni” Institute of Macromolecular Chemistry.

[‡] Chemistry Institute, Moldavian Academy.

* To whom correspondence should be addressed. E-mail: mcazacu@icmpp.ro.

derivative is used in our paper as an intermediary for obtaining siloxane-based polyamides and polyesters of the type



with $X = O$ or NH and $R =$ di- or oligosiloxane-containing linear sequences.

We chose the polycondensation procedure because this permits to use a large range of functionalized monomers. In addition, model compounds can be obtained which to help in the characterization of the polymers. It is expected that the presence of the internal polar functions (amide or ester) in polymeric structures will influence some of the properties.

The paper originality consists of obtaining the new siloxane-ferrocene polymers and evaluation of the influences of the three main parameters—siloxane length, ferrocene content, and internal function type—on their properties.

Experimental Section

Materials. Ferrocene, Fluka, mp 172–174 °C. 1,1'-Di(chlorocarbonyl)ferrocene, $ClCO-C_5H_4-Fe-C_5H_4-COCl$ (CAFc), was prepared by a three-step procedure starting from the ferrocene, according to methods described in the literature^{20,21} passing by 1,1'-diacetylferrocene obtained by Friedel–Crafts acylation of the ferrocene (40% yield), followed by oxidation to 1,1'-ferrocenedicarboxylic acid (about 80% yield), and finally conversion to diacid chloride by the treatment with oxalyl chloride (64.6% yield). The product recrystallized from petroleum ether resulted in form of red crystals melting at 95–100 °C. The presence in the IR spectrum of the strong absorption band specific for carbonyl from the $-COCl$ group at 1760 cm^{-1} is additional proof for compound formation. 1,3-Bis(aminopropyl)tetramethyldisiloxane (AP_0), supplied by Fluka, was used as received. α,ω -Bis(3-aminopropyl)oligodimethylsiloxane (AP), having an average number molecular weight of 744, was synthesized according to the known procedure²² by the bulk equilibration reaction of octamethylcyclotetrasiloxane with 1,3-bis(aminopropyl)tetramethyldisiloxane in the presence of a base, tetramethylammonium hydroxide (TMAH), as catalyst. 1,3-Bis(hydroxypropyl)tetramethyldisiloxane (HP_0) supplied by ABCR GmbH & Co was used as received. 4-Hydroxybenzaldehyde (Fluka AG) was recrystallized from water, mp 114–117 °C. Oxalyl chloride, OC (Fluka), bp 62–65 °C, $d_4^{20} = 1.5$. Pyridine (Fluka) was used as received. Methylene chloride was dried by refluxing over CaH_2 and freshly distilled before use.

Equipment. The IR spectra were recorded on a SPECORD M80 spectrophotometer. The 1H NMR and ^{13}C NMR spectra were recorded on a Bruker Avance DRX 400 spectrometer, using $DMSO-d_6$ or $CDCl_3$ as solvents and tetramethylsilane as an internal standard.

Electronic absorption spectra were measured using a SPECORD M42 spectrophotometer with quartz cells of 1 cm thickness in different solvents.

UV irradiation was carried out with a 350 W mercury arc lamp at room temperature. The reduced viscosities of polymer solution (0.5% w/v) in NMP or NMP/ CH_3OH mixture were determined at 25 °C using an Ubbelohde suspended level viscometer.

Polarized light optical microscopy (POM) observations were made with an Olympus BH-2 microscope (Japan), equipped with a THMS 600/HSF9I hot stage.

Transmission electron micrographs were obtained on a TESLA 513 A electron microscope. Polymer, as a solution ca. 0.1% in THF,

was sprayed onto a thin carbon film grown on collodium placed on a copper TEM grids.

Gel permeation chromatographic analysis (GPC) was carried out on a PL-EMD 950 evaporative mass detector instrument by using DMF as eluant after calibration with standard polystyrene samples.

Thermogravimetric measurements were performed in air at a heating rate of 10 °C/min in air using a Q-1500D System (F. Paulik, J. Paulik, Erdey).

The DSC analyses were done on a Mettler TA DSC 12E Instrument, with heating and cooling rate of 10 °C/min.

The magnetic properties were evaluated by using a homemade magnetometer with vibrating sample, at an applied field of 70 kOe.

The redox activity of the synthesized ferrocene-containing polymers was investigated by differential pulse voltammetry using a Polarograph PA-3 in pulse differential regime (5 impulses/s) and an impulse amplitude of 25 mV. The scan rates $\nu = 10$ –50 mV/s. DMF was used as a solvent and 0.1 M solution of $NaClO_4$ as the electrolyte. The working electrode has been prepared from carbon fiber UMV-30 (1800 °C, 30 μm in diameter).

The silicon content was determined according to an adapted procedure:²³ disintegration with sulfuric acid and ignition at 900 °C to constant weight. Finally, the residue was treated with HF for silicon removal as SiF_4 and then calculation by difference. The iron content was determined from the residue remained after silicon analysis, considering that Fe_2O_3 is formed.

Procedures. *Siloxane Derivative. Preparation of Bis-phenolic siloxane-azomethine Macromer (HBSO).* 2.44 g (0.02 mol) of 4-hydroxybenzaldehyde and 2.48 g (0.01 mol) of AP_0 were together dissolved in 50 mL of methanol. The mixture was refluxed 9 h. After partial solvent removing and cooling, the mixture was poured in a large water excess to precipitate the azomethine, which was then separated by filtration, washed with warm water and petroleum ether, dried, weighed, and analyzed. The azomethine was isolated as a yellow-brown film. Yield: 40%.

Polycondensation. Synthesis of the Siloxane-Containing Polymers with/without Ferrocene. In a well-dried one-necked flask equipped with a magnetic stirrer and nitrogen inlet, diacid chloride (oxalyl or ferrocene) was dissolved in freshly dried CH_2Cl_2 for a solution of about 50 wt % concentration. AP_0 or AP in molar ratio 1:1 toward diacid chloride and pyridine in excess was added. The reaction mixture was stirred in ice bath for about 1 h and, until 24 h, at room temperature, although the chlorohydrate as a white precipitate appeared just in the first 1–2 h. Finally, the reaction mixture was filtered off in order to separate the pyridine chlorohydrate. The filtrate was repeated washed with water in separation funnel, dried on anhydrous sodium sulfate, and filtered, and the solvent was removed by a rotavapor. The polymer was dried over P_2O_5 in a vacuum. An orange or dark-brown transparent film was obtained and characterized.

By using 1,3-bis(hydroxypropyl)tetramethyldisiloxane or 1,3-bis(*p*-hydroxyphenyleneazomethine-3-propyl)tetramethyldisiloxane as a siloxane partner, in the same way, the properly polyesters as an orange viscous oil or film, respectively, have been obtained. However, the polyesterification reactions occurred somewhat slowly. Therefore, they have been led without cooling at room temperature. The polymers were purified by reprecipitation with hexane from methylene chloride solution.

Preparation of the Siloxane-Containing Polyamide Doped with Ferrocene (SAFd). 0.302 g (1 mmol structural units) of siloxane-based polyamide without ferrocene, POA, dissolved in 10 mL of THF was mixed with a 5 mL solution containing 0.369 g (1 mmol) of ferrocene in THF and stirred in the dark for about 3 h. Then, the solvent was removed in a vacuum. The product resulted as a light orange film with uniform, homogeneous aspect observed by POM at a magnitude of 400. By TEM investigation, a diffraction image consisting of bright spots that can be assigned to the monocrystals containing ferrocene was obtained (Figure 1). On the basis of the microphotography, it can be appreciated that a nanoscale dispersion of ferrocene in polymeric matrix occurred.

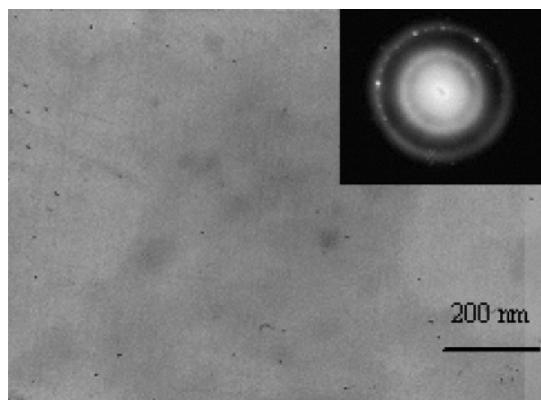
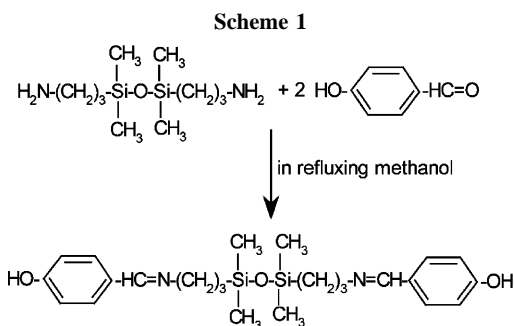


Figure 1. TEM image of SAFd (inset: small area electron diffraction pattern).

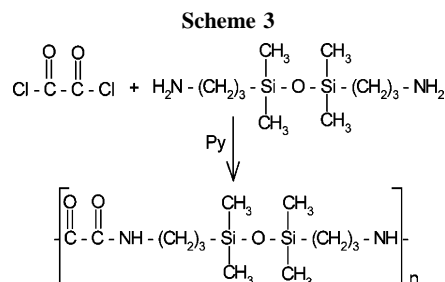
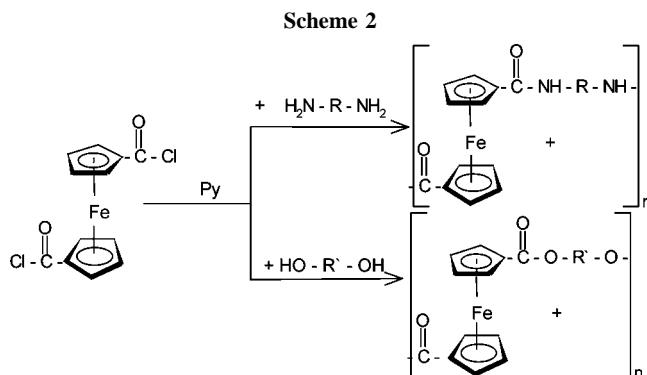


Results and Discussion

Siloxane Derivative, HBSO. A bis-phenol-containing siloxane sequence and azomethine linkages was synthesized by condensation of *p*-hydroxybenzaldehyde with 1,3-bis(3-aminopropyl)-tetramethyldisiloxane in 2:1 molar ratio, reaction occurring in refluxing methanol, according to Scheme 1. This compound was prepared in order to use it as a polycondensation comonomer with 1,1'-di(chlorocarbonyl)ferrocene.

Elemental analysis: Found (Calcd): C 62.8 (63.2), H 8.2 (7.9), N 5.9 (6.1), Si 12.9 (12.3). IR spectrum (KBr), cm^{-1} : 1640 ($\text{CH}=\text{N}$), 1590, and 830 (aromatic). Significant modifications appear in the ^1H NMR spectra of the bis-phenol azomethine compared with the reactants. ^1H NMR, in DMSO, σ (ppm): 9.7 ($-\text{CH}=\text{N}-$), 8.1, 7.7, and 7.5 (aromatic CH), 3.4 ($\text{Si}(\text{CH}_2)_2-\text{CH}_2-\text{N}=\text{C}$), 1.6 ($\text{Si}-\text{CH}_2-\text{CH}_2-\text{CH}_2-\text{N}=\text{C}$), 0.5 ($\text{Si}-\text{CH}_2-(\text{CH}_2)_2-\text{N}=\text{C}$), and 0.05 ($(\text{CH}_3)_2\text{Si}-\text{O}$). The product is soluble in CHCl_3 , acetone, DMF, DMSO, THF, and NMP and insoluble in petroleum ether, benzene, and toluene.

Synthesis of the Polymers. In the present paper we prepared polyamides and polyesters containing strictly alternating ferrocene units and siloxane sequences by polycondensation of the proper precursors in solution, at low temperature in order to avoid undesirable side reactions. The difunctional ferrocene derivative was used as a diacid chloride for activation of the polycondensation process. The used siloxane precursors were 1,3-bis(3-aminopropyl)tetramethyldisiloxane (AP_0), α,ω -bis(3-aminopropyl)oligodimethylsiloxane (AP), 1,3-bis(3-hydroxypropyl)tetramethyldisiloxane (HP_0), and 1,3-bis(*p*-hydroxyphenyleneazomethyne-3-propyl)tetramethyldisiloxane (HBS_0). The polycondensations (Scheme 2) occurred in methylene chloride as a solvent and pyridine as hydrochloric acid acceptor. The reactions have been proved to be effective and very fast. The polyamidation reaction is almost instantaneous and exothermic, and therefore this was carried out in ice bath. However, the polyesterification occurs somewhat slowly, and therefore, it has been performed at room temperature, without cooling. The



ferricinium ion formation was observed when a stoichiometric quantity of pyridinium was added. Therefore, pyridine excess was necessary.

To identify and explain the ferrocene contribution on certain properties of the siloxane-ferrocene polymers, a model polyamide without ferrocene (SA) was synthesized, according to Scheme 3. The resulting polymers (Table 1) were characterized by elemental analysis, viscometry, GPC, UV-vis spectrophotometry (Table 1), DSC, POM, ^1H NMR, and IR spectra.

The disiloxane-containing polyamide SAF1 is a solid. As the length of the chain between the ferrocene units increases (i.e., oligosiloxane), the softening point of the polymer decreases and a waxlike polymer, SAF2, is obtained. The polyester, even based on disiloxane sequences (SEF1), is a liquid. When azomethine groups are also present in the chain, the polyester (SEF2) is a solid. These differences in the polymer aspect can be explained by the hydrogen bonds developed in the polymers containing amide or azomethine groups.

Elemental analysis values for silicon and iron contents in polymers were found in agreement with the proposed structures (Table 1). These elements were chosen as the most reliable in order to verify the structures because, as already reported,^{11,18} the other elements led to nonreproducible values. This was explained by the ceramic product formation in the analysis conditions.

The obtained polymers were soluble in common organic solvents as shown by the results presented in Table 2. Reasonable values of the reduced viscosity, taking into account the presence of the highly flexible siloxane sequences, were obtained. The number-average molecular mass (M_n) values estimated by GPC were in the range 2700–14 200 and polydispersity index 1.1–2.1 (Table 1). The polycondensation reaction occurrence was confirmed by IR spectroscopy. Thus, the acid chloride $\text{C}=\text{O}$ peak at 1760 cm^{-1} disappears, coincident with the appearance of the amide or ester absorption bands. In the SAF1 spectrum (Figure 2a), a very strong carbonyl stretching vibration is present at 1630 cm^{-1} assigned as being an amide I band. The amide II band is evident near 1540 cm^{-1} and amide III band at 1285 cm^{-1} .²⁴ In addition, ferrocene $\text{sp}^2 \text{ C}-\text{H}$ stretching occurred around 3100 cm^{-1} and asymmetric and

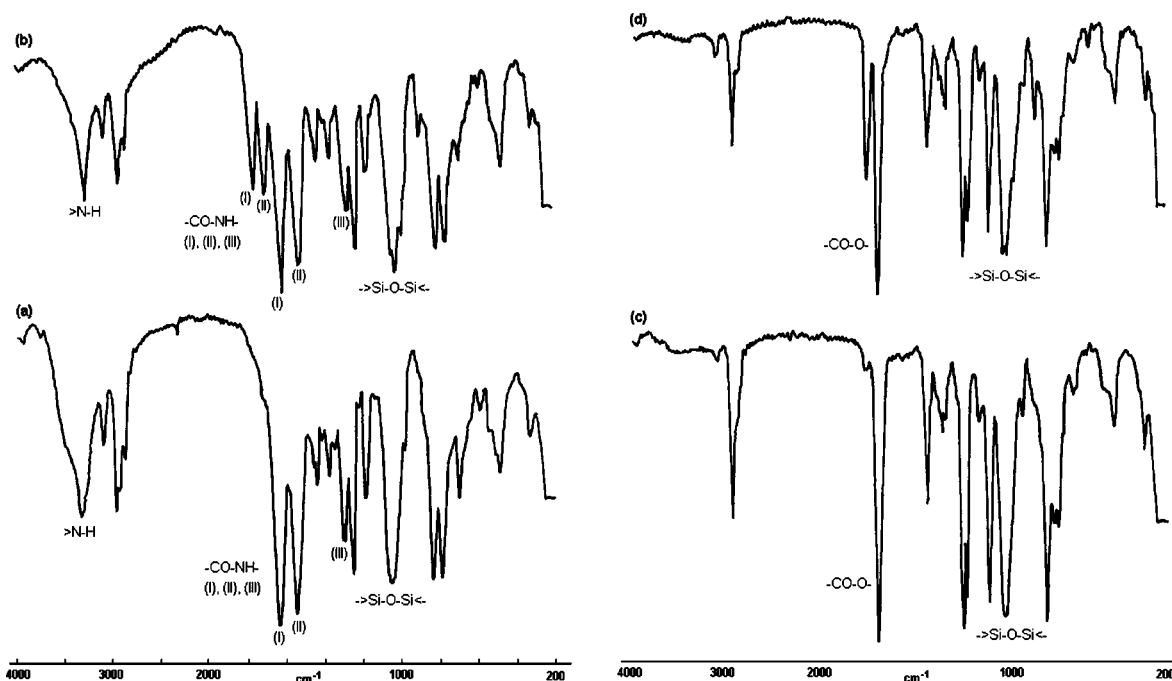


Figure 2. Representative IR spectra for polyamide SAF1 (a, unoxidized; b, oxidized form) and polyester SEF1 (c, unoxidized; d, oxidized form).

Table 1. Some Analytical Data for the Synthesized Ferrocene-Containing Polymers

sample	reactants	elem anal., %, found/calcd ^a		$\eta_{\text{red}}^{25}/\text{solvent},^d \text{ dL/g}$	GPC data ^e		
		Si ^b	Fe ^c		M_n	I	λ , nm (in CHCl_3)
SAF1	CAFc + APo	10.6/11.5	10.9/11.5	0.78/NMP + MeOH	14200	1.2	442
SAF2	CAFc + AP ₁₅	25.0/24.1	5.4/6.0	0.50/NMP	8800	1.3	437
SA	OC + APo	17.9/18.5		1.38/NMP	11800	2.1	
SEF1	CAFc + HPO	10.2/11.4	11.5/11.4	0.31/NMP	2700	1.1	453
SEF2	CAFc + HBSO	7.8/8.1	7.9/8.1	0.64/NMP	5700	1.2	430

^a Calculated for the presumed structural unit; uninvestigated. ^b Determined according to ref 23. ^c Determined from the residue remained after silicon analysis, considering that Fe_2O_3 is formed. ^d Determined for a concentration of about 0.5 g/dL. ^e Measured in DMF, for a concentration of about 1 g/dL.

Table 2. Solubilities of the Obtained Polymers^a

sample	DMF	THF	DMSO	CH_3OH	CHCl_3	acetone	NMP	CH_2Cl_2
SAF1	+	—	+	+	+	—	+	+
SAF2	+	+	+	—	+	—	+	+
SA	+	+	+	—	+	+	+	+
SEF1	+	+	+	+	+	+	+	+
SEF2	+	+	+	—	+	—	+	+

^a — insoluble; + — partially soluble; + soluble.

symmetric sp^3 C—H stretching at 2950 and 2860 cm^{-1} , respectively. The polyamide exhibited a broad, intense N—H stretching vibration around 3300 cm^{-1} .²⁵ The polyester SEF1 showed the carbonyl absorption near 1715 cm^{-1} (Figure 2b). For SEF2 the carbonyl absorption appears at 1700 cm^{-1} . The azomethine absorption band of polymer SEF2 at about 1640 cm^{-1} and aromatic absorptions at 1600 and 800–750 cm^{-1} were also evidenced in the IR spectrum.

Supplementary bands appeared for carbonyl absorption for both ferrocene-containing polyesters (1780 cm^{-1} for SEF1 and 1740 cm^{-1} for SEF2) and polyamides (1780 and 1715 cm^{-1} assigned to amide I and amide II, respectively), when ferricinium ion is formed (Figure 2c,d). These shifts of the $\nu(\text{C}=\text{O})$ band to higher frequencies were justified¹⁸ by oxidation of ferrocenyl moieties which inductively withdraws electrons from the amide or ester groups directly attached to the cyclopentadienyl ring and thus increases the strength of the C=O bands. For all

polymers the characteristic absorption bands assigned to the siloxane sequence 1000–1100 (Si—O—Si), 800, 1260 cm^{-1} (Si—CH₃) are visible in the IR spectra.

¹H NMR. As other authors have already observed in similar studies,¹¹ the traces of paramagnetic impurities as result of oxidation of ferrocene to ferricinium derivative causes a broadening of the peaks in NMR spectra. Thus, the ¹H NMR spectrum of the polyamide SAF1 (in CDCl_3) shows two broad resonances for the two sets of cyclopentadienyl protons at 4.26–4.39 and 4.71–4.83 ppm, besides the protons from $-\text{CH}_2-\text{CH}_2-\text{CH}_2-\text{Si}\equiv$ at 3.16, 1.52, and 0.54 ppm and $(\text{CH}_3)_2\text{Si}\equiv$ at 0.063 ppm. The amidic proton resonance is visible at about 8.0 ppm.

In polyester SEF1 the resonance for cyclopentadienyl protons are still broader: 4.37–4.62 and 4.79–4.99 ppm. The signals for methylene protons, $-\text{CH}_2-\text{CH}_2-\text{CH}_2-\text{Si}\equiv$, are assigned at about 3.77, 1.70, and 0.59 ppm, respectively. The proton's

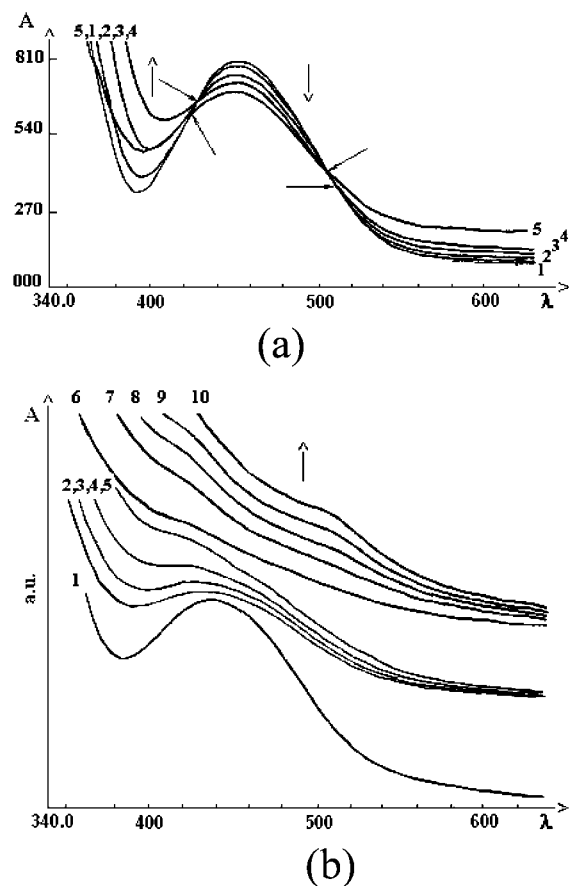


Figure 3. UV-vis spectra for (a) SEF1 in CHCl_3 (1, initial sample; 2, 3, 4, 5, irradiated after 4 min, 12 min, 20 min, and 70 min, respectively); (b) SAF1 in NMP (1, initial sample; 2, 3, 4, 5, 6, 7, 8, 9, 10, irradiated after 15 s, 30 s, 1 min, 2 min, 5 min, 21 min, 40 min, 67 min, and 94 min, respectively).

resonance from $(\text{CH}_3)_2\text{Si}=\text{}$ groups is visible at about 0.075 ppm. The ^1H NMR spectrum for SEF2 reveals in addition signals at 8.3–8.1 ppm for $\text{CH}=\text{N}-$ and 7.2–6.8 ppm for aromatic CH. The chemical shifts corresponding to the protons from $(\text{Si}(\text{CH}_2)_2-\text{CH}_2-\text{N}=\text{C})$ are visible at 3.9–3.7 ppm compared to 2.7–2.4 ppm for $(\text{Si}(\text{CH}_2)_2-\text{CH}_2-\text{N}=\text{C})$ in 1,3-bis(3-amino-propyl)tetramethyldisiloxane. The ratios of the resonances have the expected values.

UV-vis absorption spectra reveal the presence of the absorption band at about 430–450 nm (Table 1) assigned to d–d electronic transitions of the ferrocenyl groups in polymers.²⁷

The photobehavior of the synthesized polymers was studied in different solvents (chloroform, dimethylformamide, *N*-methylpyrrolidone) following the modifications occurring in the intensity of the absorption band at 440–450 nm during UV light irradiation. The UV irradiation of SEF1 in chloroform solution determines the decrease of the absorbance at 453 nm (Figure 3a). In the first stages of the photoprocess, two isosbestic points can be observed at 436 and 503 nm, respectively. At the same time, the maximum of this absorption band exhibits a shift to shorter wavelengths, and a new absorption band is developed at about 640 nm due to the ferricinium cation formed during irradiation. As a result, at higher irradiation times, the absorption curves do not intersect the others in the two isosbestic points. By keeping the solution for 15 days at room temperature, no modification occurred in the absorption spectrum.

In electronic absorption spectra of SEF2 in chloroform, the ferrocene absorption band appears as a shoulder at 430 nm, besides those characteristic for azomethine group, as a shoulder,

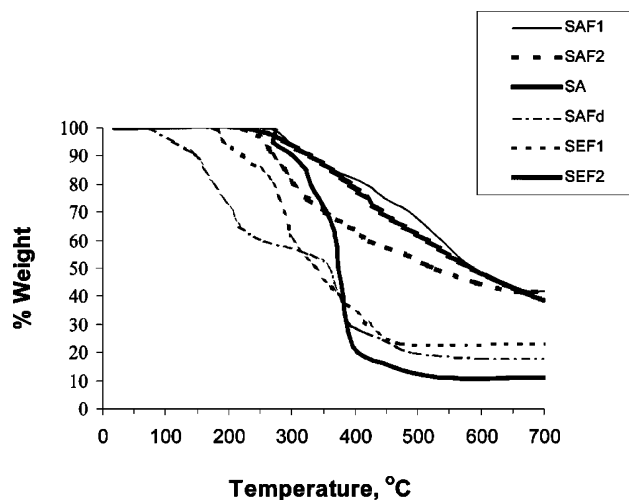


Figure 4. Comparative TGA curves for the synthesized polymers.

at 315 nm and aromatic ring as an intense band at 257 nm. During irradiation, the ferrocene band increases in intensity, the shoulder becoming broader and faint. The same trend is also found for the azomethine band.

For the sample SAF1 in chloroform solution, the absorbance at 442 nm also decreases with irradiation time without isosbestic points in spectra, and after 55 min, the absorption band at 442 nm became a shoulder. The absence of isosbestic points and this spectral pattern due to UV irradiation showed that during irradiation more photoprocesses can take place.

The spectral pattern of SAF2 in chloroform is similar to SEF2 sample. In contrast to the chlorinated solutions, the sample SEF1 irradiated in aprotic dipolar solvents exhibit a different spectral pattern. With increased irradiation times, the spectral curves display an increased absorption throughout the spectral region under study. Thus, after 2 min of irradiation the absorption band at 438 nm for SAF1 in NMP solution becomes shoulder (Figure 3b). At high irradiation times new absorption bands were developed at about 510 and 660 nm, respectively. This process occurs more rapidly in DMF solutions. Like as in the electrochemical behavior, it can be appreciated that the photochemical response is more slowly for polyesters than for polyamides.

Following the molecular weight values before and after UV irradiation it could be appreciated that some degradation occurs. For example, after irradiation for 1 h, the M_n value of SEF2 decreased from 5600 to 4800. However, more complex processes may occur under UV irradiation, which would require thorough investigation.

The thermal stability of the copolymers was evaluated by thermogravimetric analysis (TGA) performed in air at a heating rate 10 °C/min. The curves are shown in Figure 4, most of them revealing a multistage process, as was also emphasized by Souza et al.,²⁸ who investigated the thermal degradation of some ferrocene-containing polyamides.

A general trend that can be observed from the TGA data is that the polymers having amide-linked ferrocenyl moieties are more stable than the polyamide without ferrocene because of the increased thermal stability induced by the linked ferrocene presence. The thermal stability decreases when the siloxane sequence length increases. Therefore, we could assume that the siloxane part is the first to decompose in these compounds. The polymer with ester-linked ferrocenyl moieties is less stable than the polyamide. The hydrogen bonding between amide linkages in the polyamides can explain this behavior. The same good thermal stability can be also observed in the case of the polyester

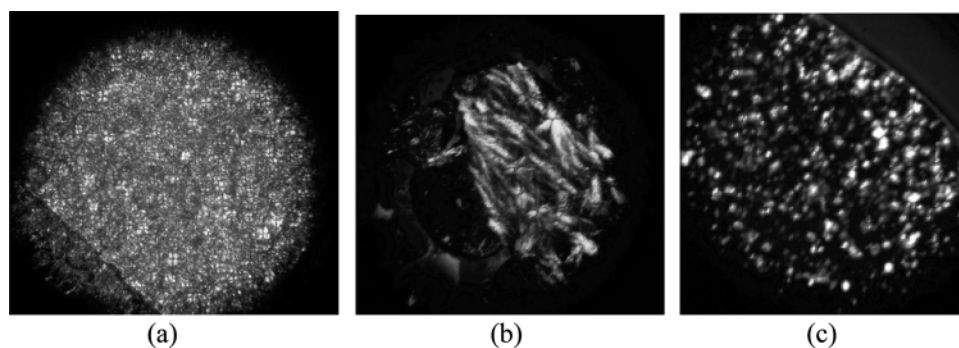


Figure 5. POM microphotographs, crossed polarizers, 200 \times : (a) SA, 62 $^{\circ}\text{C}$; (b) SAF1, 146 $^{\circ}\text{C}$; (c) SEF2, 83 $^{\circ}\text{C}$.

Table 3. Main Thermogravimetric Data for the Synthesized Polymers

sample	T_{10}^a	T_{40}^a	T_f^b	% residue
SAF1	330	538	673	42
SAF2	268	424	655	42
SA	302	370	535	11
SAFd	146	255	599	18
SEF1	221	302	473	23
SEF2	330	517	>700	39 ^c

^a Temperature for 10% and 40% weight loss, respectively. ^b Final decomposition temperature. ^c Incomplete decomposition.

having azomethine beside ester linkages where the hydrogen bonding is also possible. The free ferrocene presence in doped polyamide, SAFd, has as a result a decrease in the thermal stability relative to the simple polyamide, SA. In this case, the ferrocene probably catalyzes the thermal decomposition of polymer.²⁹

Some data derived from TG curves are shown in Table 3. The TGA residues in air present magnetic properties. For example, the magnetization, σ , of the TGA residue for the SAF1 sample at an applied field of 70 kOe is 14 emu/g. We will investigate the magnetic properties of the thermally treated polymers in a further paper.

Mesomorphic Properties. The thermotropic LC behavior of polyamides SA and SAF1 and polyester SEF2 was investigated by POM and DSC. A good correlation for the main transition temperatures, i.e., melting (T_m) and clearing (isotropization, T_{iz}), was obtained by the two methods.

SA (without ferrocene) melted at 60 $^{\circ}\text{C}$ and exhibited a texture with schlieren disclinations, as shown in Figure 5a. The clearing process was rather slow both in POM observations and in DSC (first heating scan) and was completed at 145 $^{\circ}\text{C}$, as can be seen in Figure 6a. On cooling, the sample did not organize completely, although the same texture was observed the next day in some areas of the preparation.

The ferrocene-containing polyamide SAF1 exhibited higher transition temperatures, as presented in Figure 6b,c: T_g 65 $^{\circ}\text{C}$, T_m 120 $^{\circ}\text{C}$, T_{iz} 175 $^{\circ}\text{C}$ (190–200 $^{\circ}\text{C}$ by POM). The POM did not reveal a classical texture in the LC phase, as shown in Figure 5b, and no birefringence was noticed on cooling.

As can be seen from the chemical structure of the two polyamides, they do not contain mesogenic groups; nevertheless, they showed crystalline order and melting birefringence in POM. On the other hand, the polyester SEF1, with similar constituent segments as SAF1, is an isotropic liquid at room temperature. This quite different behavior could be due to the strong intermolecular H-bondings in polyamides, which provide a supramolecular assembly.

The polyester SEF2 revealed a fine granular texture in molten state on POM observation (Figure 5c), and rather low transition temperatures, as observed by DSC (Figure 6d) and confirmed

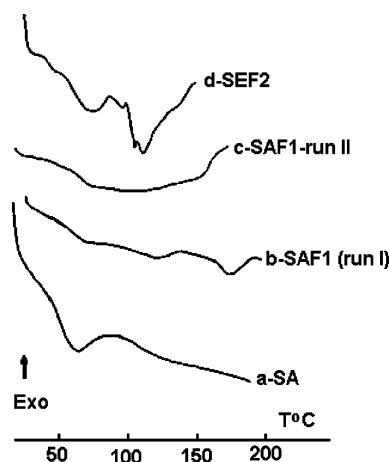


Figure 6. DSC scans of SA, first heating (a), SAF1, first heating (b), SAF1, second heating (c), and SEF2, first heating (d).

by POM: T_g 50 $^{\circ}\text{C}$, T_m 75 $^{\circ}\text{C}$, T_{iz} 108 $^{\circ}\text{C}$. The same observation was made on cooling; i.e., the sample did not organize at the usual cooling rate. However, when observed after a few days, the sample was crystalline, which shows very slow ordering.

The redox activity of the synthesized ferrocene-containing polymers was investigated by differential pulse voltammetry.

All studied polymers exhibited a single quasi-reversible oxidation process, suggesting that the oxidation of all ferrocenyl moieties occurred at the same potential. An illustrative differential pulse cyclic voltammogram is presented in Figure 7. In the anodic–cathodic scan, the anodic current was higher than the cathodic one. However, the two currents became equal in intensity in the cathodic–anodic scan. A possible explanation would be an autocatalyzed spontaneous reduction process from Fe^{3+} to Fe^{2+} because of the higher stability of the reduced form in comparison with the oxidized one.

The detection of a single reversible oxidation wave indicates that in these polymers the iron centers are essentially noninteracting. Such behavior has already been reported for some ferrocene-containing polymers in which, as in our case, the redox-active centers are separated from one another by large silicon-containing chains with insulating organic units.¹⁸

The main electrochemical data for some synthesized polymers are presented in Table 4. In the systems having linked ferrocenyl units, the ΔE conversion potential value is dependent on both the length and nature of the bridge between the metal centers, as has already been observed.²⁶ However, between polyamides SAF1 and SAF2, which differ by the siloxane sequences length, very close values for ΔE were obtained. This can be explained by the fact that the disiloxane segment is enough to completely impede ferrocene units interaction so that the increase of the siloxane segment cannot additionally influence the redox

Table 4. Differential Pulse Voltammetry Data for Some Ferrocene-Containing Polymers^a

sample	E_p^c , mV	E_p^a , mV	ΔE_p , mV	$\Delta E_p/2$, mV	I_p^c , mA/(g/mL)	I_p^a , mA/(g/mL)
SAF1	880 ± 20	938 ± 20	60 ± 20	188 ± 10	0.11 ± 0.01	0.34 ± 0.01
SAF2	880 ± 20	960 ± 20	80 ± 20	175 ± 10	0.09 ± 0.01	0.28 ± 0.01
SAFd	553 ± 15	677 ± 15	124 ± 15	338 ± 10	0.56 ± 0.01	0.52 ± 0.01
SEF1	1114 ± 10	1193 ± 10	79 ± 10	288 ± 10	0.12 ± 0.01	0.23 ± 0.01
SEF2	1000 ± 10	1100 ± 10	100 ± 10	275 ± 10	0.14 ± 0.01	0.39 ± 0.01

^a E_p^c , I_p^c = potential, current cathodic values. E_p^a , I_p^a = potential, current anodic values. $\Delta E_p = E_p^a - E_p^c$. $\Delta E_p/2$ = width of anodic peak at its semiheight.

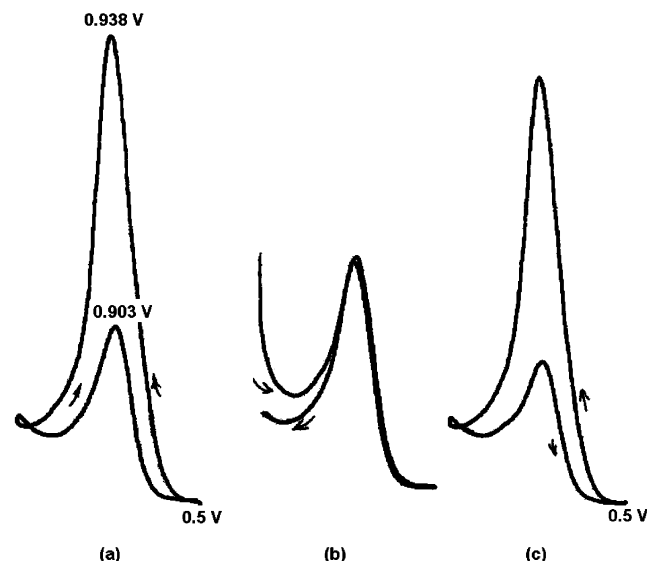


Figure 7. Differential pulse voltammograms of polymer SAF1 at a glassy carbon rod electrode in DMF/0.1 M NaClO₄ solution: (a) anodic-cathodic scan; (b) cathodic-anodic scan; (c) repeated anodic-cathodic scan.

potential. Some differences, although small enough, can be observed in the anodic (I_p^a) and cathodic (I_p^c) currents values for SAF1 and SAF2. As expected, by increasing the segment length between ferrocene units, the current value decreases due to the lowering of the relative ferrocene content in polymer.

When comparing a polyamide and polyester having the same siloxane sequence length between metal centers, more significant differences in ΔE values can be observed, namely a shifting to more anodic peak current in the case of polyester SEF1 toward polyamide SAF1. In the same time, the peak width indicates that the ferrocene redox conversion in SEF1 occurs more slowly (electrochemical irreversibility increases). This trend is also visible when comparing values of the anodic and cathodic currents for the two compounds. In SEF2 the redox conversion more easily occurs, as compared with SEF1.

The polyamide doped with ferrocene behaves very differently as compared with the polymers containing chemically linked ferrocene units. The conversion potential range is shifted 300–600 mV to cathodic. The anodic and cathodic current peaks are almost identical. However, the width of the anodic and cathodic semipeaks exceeds the values determined for the other studied polymers. This can be justified by the absence of the chemical linkage between ferrocene and polyamide. The strong electron-withdrawing effect of the carbonyl group on the ferrocenyl moiety, when directly bound to the cyclopentadienyl ring, makes the polymer more difficult to oxidize, as was explained by Casado and co-workers¹⁸ for polyamides.

A noteworthy aspect of the redox behavior for all studied ferrocene-linked polymers is their ability to modify glassy electrode surfaces, resulting in detectable electroactive films that remain persistently attached to the electrode surface, even untreated. As a result, these copolymers can be electrodeposited

in their oxidized forms onto electrode surfaces. This is illustrated by decreasing both anodic and cathodic currents after repeated cycles (Figure 6c). Such behavior (the ferrocene adsorption on the electrode) was not observed in the case of doped polyamide, SAFd.

Conclusion

Some new linear polymeric structures containing amide or ester-linked alternating siloxane sequences and ferrocene units in the backbone have been synthesized and characterized. All polymers are soluble in common organic solvents and have high values of the reduced viscosity compared to other polymers containing highly flexible siloxane sequences.

The ferrocene units confer high thermal stability and redox activity. The siloxane units improve solubility and decrease the transition temperatures. The presence of ester, amide, or azomethine internal functions influences most of the copolymer's behaviors (thermal, mesomorphic, photochemical, and redox); thus, the linkage type between the two comonomer units can be used as a parameter in designing compounds with desired properties. The electrochemical behavior of the synthesized polymers suggests their potential application in the chemical modification of the electrodes.

References and Notes

- (1) Manners, I. *Pure Appl. Chem.* **1999**, *71*, 1471–1476.
- (2) Manners, I. *J. Polym. Sci., Part A: Polym. Chem.* **2002**, *40*, 179–191.
- (3) Cyr, P. W.; Tzolov, M.; Manners, I.; Sargent, E. H. *Macromol. Chem. Phys.* **2003**, *204*, 915–921.
- (4) Noll, W. *Chemistry and Technology of Silicone*; Academic Press: New York, 1968; p 437.
- (5) Gupta, K. C.; Abdul Kadir, H. K.; Chand, S. J. *Macromol. Sci., Pure Appl. Chem.* **2002**, *A39*, 1451–1474.
- (6) Rehahn, M. *Acta Polym.* **1998**, *49*, 201–224.
- (7) Fryzuk, M. D.; Leznoff, D. B.; Ma, E. S. F.; Rettig, S. J.; Young Jr., V. G. *Organometallics* **1998**, *17*, 2313–2323.
- (8) Najafi-Mohajeri, N.; Nelson, G. L.; Benrashed, R. *J. Appl. Polym. Sci.* **2000**, *76*, 1847–1856.
- (9) Abd-El-Aziz, A. S. Overview of Organoiron Polymers. In *Macromolecules Containing Metal and Metal-like Elements*; Abd-El-Aziz, A. S., Carraher Jr., C. E., Pittman Jr., C. U., Sheats, J. E., Zeldin, M., Eds.; John Wiley & Sons: New York, 2004; Vol. 2, pp 1–27.
- (10) Alonso, B.; Gonzalez, B.; Garcia, B.; Ramirez-Oliva, E.; Zamora, M.; Casado, C. M.; Cuadrado, I. *J. Organomet. Chem.* **2001**, *637*–639, 642–652.
- (11) Sargent, J. R.; Weber, W. P. *Polymer* **1999**, *40*, 3795–3802.
- (12) Ni, Y.; Rulkens, R.; Manners, I. *J. Am. Chem. Soc.* **1996**, *118*, 4102–4114.
- (13) Power-Billard, K. N.; Manners, I. *Macromol. Rapid Commun.* **2002**, *23*, 607–611.
- (14) Losada, J.; Garcia Armada, M. P.; Cuadrado, I.; Alonso, B.; Gonzalez, B.; Casado, C. M.; Zhang, J. *J. Organomet. Chem.* **2004**, *689*, 2799–2807.
- (15) Boudjouk, P.; Al-Badri, Z. M. H.; Chauhan, B. P. S. *J. Organomet. Chem.* **2004**, *689*, 3468–3471.
- (16) Garcia Armada, M. P.; Losada, J.; Cuadrado, I.; Alonso, B.; Gonzalez, B.; Casado, C. M. *Electroanalysis* **2003**, *15*, 1109–1114.
- (17) Patterson, W. J.; McManus, S. P.; Pittman Jr., C. U. *J. Polym. Sci. Chem. Ed.* **1974**, *12*, 837–850.
- (18) Casado, C. M.; Moran, M.; Losada, J.; Cuadrado, I. *Inorg. Chem.* **1995**, *34*, 1668–1680.
- (19) Pittman Jr., C. U. *J. Polym. Sci., Part A-1: Polym. Chem.* **1968**, *6*, 1687–1695.

- (20) Vogel, M.; Rausch, M.; Rosenberg, H. *J. Organomet. Chem.* **1957**, 22, 1016–1018.
- (21) Knobloch, F. W.; Rauscher, W. H. *J. Polym. Sci.* **1961**, 51, 651–656.
- (22) Hedrick, J. L.; Haidar, B.; Russel, T. P.; Hofer, D. C. *Polym. Prepr.* **1987**, 28, 99.
- (23) Gaul, M. D.; Angelotti, N. C. In *The Analytical Chemistry of Silicones*; Smith, A. L., Ed.; Wiley: New York, 1991; p 181.
- (24) Neuse, E. W.; Rosenberg, H. *J. Polym. Sci., Part A-1* **1968**, 6, 1567–1582.
- (25) Gonsalves, K.; Zhan-ru, L.; Rausch, M. *J. Am. Chem. Soc.* **1984**, 106, 3862–3863.
- (26) Pudelski, J. K.; Foucher, D. A.; Honeyman, C. H.; Macdonald, P. M.; Manners, I.; Barlow, S.; O'Hare, D. *Macromolecules* **1996**, 29, 1894–1903.
- (27) Sohn, Y. S.; Hendrickson, D. N.; Gray, H. B. *J. Am. Chem. Soc.* **1971**, 93, 3603–3612.
- (28) De Souza, A. C.; Pires, A. T. N.; Soldi, V. *J. Therm. Anal. Calorim.* **2002**, 70, 405–414.
- (29) Barry, A. J.; Beck, H. N. Siloxane Polymers. In: *Inorganic Polymers*; Stone, F. G. A., Graham, W. A. G., Eds.; Academic Press: New York, London, 1962; p 272.

MA052030Y